J. Plasma Physics (2003), *vol.* 69, *part* 5, *pp.* 397–412.
DOI: 10.1017/S0022377803002241 Printed in the United Kingdom

Degenerate continuous spectra producing localized secular instability – an example in a non-neutral plasma

M. HIROTA, T. TATSUNO and Z. YOSHIDA

Graduate School of Frontier Sciences, University of Tokyo, Tokyo 113-0033, Japan
(hirota@plasma.q.t.u-tokyo.ac.jp)

(Received 3 June 2002 and in revised form 30 November 2002)

Abstract. Fluctuations in ambient shear flow exhibit interesting transient phenomena. Shear flow produces not only Kelvin–Helmholtz modes (global exponential instabilities represented by point spectra) but also local algebraic instabilities associated with multiple continuous spectra. Since the generating operator is non-Hermitian, the orthogonality of eigenmodes is broken, and unresolvable mode couplings (resonances) bring about secular behavior (algebraic instability). We analyze electrostatic fluctuations in a magnetized non-neutral (single species) plasma where the electrostatic potential parallels the stream function. This secular behavior is reproduced by solving the initial value problem with a renormalization method.

1. Introduction

Transient phenomena in a non-Hermitian system are far richer than those in a Hermitian system. The notion of a 'mode' is no longer essential when we cannot reduce the dynamical system to a complete set of independent (orthogonal) integrable dynamics of modes. The aim of this paper is to explore, with invoking an appropriate renormalization technique, the time-asymptotic behavior of secular (algebraic) modes associated with degenerate (frequency overlapping) continuous spectra. A shear flow brings about non-Hermitian properties, and also produces an essential singularity generating a continuous spectrum [1]. We consider a simple model of a magnetized non-neutral plasma, where the self-electric field drives a flow in the direction perpendicular to the magnetic field. A spatially localized electrostatic instability [2] is the subject of our analysis.

Generating an 'exponential function' of an operator is the central problem of linear theories. The behavior of such an exponential function, however, can be very different from the elementary exponential function of numbers. The phase mixing damping (well-known as the Landau damping of Langmuir waves [3, 4]) is one of the most striking observations of complex behavior of exponential functions in infinite-dimensional function spaces. We must include continuous spectra, in addition to point spectra (eigenvalues), to complete the spectral resolution of a general Hermitian operator, which describes damping (not necessarily exponential) even though all spectra of a Hermitian operator are, by definition, real. The general spectral resolution theory in function spaces (the Von Neumann theorem), however, applies only for Hermitian operators. The exponential function of a non-Hermitian

operator may exhibit much more complicated evolution, because couplings of non-orthogonal modes occur [5–7].

A simple example of finite-dimensional dynamics reveals the essential nature of such mode couplings. A linear map $\mathscr{H}$ (which may be non-Hermitian) on a finite-dimensional vector space can be cast into a Jordan canonical form; by a regular map P, we can transform

$$P^{-1}\mathscr{H}P = \mathscr{J}_1 \dotplus \mathscr{J}_2 \dotplus \cdots \dotplus \mathscr{J}_\nu, \tag{1}$$

where $\dotplus$ denotes the direct sum of linear maps, and each $\mathscr{J}_j$ is a Jordan block corresponding to an eigenvalue λ_j ($(\lambda_j I - \mathscr{J}_j)$ is a nilpotent map of class N_j, i.e. $(\lambda_j I - \mathscr{J}_j)^{N_j} = 0$), which is represented by the Jordan matrix of dimension N_j,

$$\mathscr{J}_j = \begin{pmatrix} \lambda_j & 1 & 0 & 0 \\ 0 & \ddots & \ddots & 0 \\ & \ddots & \ddots & 1 \\ 0 & & 0 & \lambda_j \end{pmatrix}. \tag{2}$$

When $\mathscr{H}$ is a normal map, all N_j are unity. Then, $\mathscr{H}$ can be diagonalized, and all modes (eigenvectors) are decoupled. A Jordan block of dimension $\geqslant 2$ represents 'unresolvable' interactions among modes. Writing

$$e^{-it\mathscr{H}} = e^{-it\lambda_j} e^{it(\lambda_j I - \mathscr{H})} = e^{-it\lambda_j}\left[I + it(\lambda_j I - \mathscr{H}) - \frac{t^2(\lambda_j I - \mathscr{H})^2}{2} + \cdots\right], \tag{3}$$

we find that $e^{-it\mathscr{H}}$ acting on the generalized eigenspace (root vectors) belonging to λ_j includes factors

$$e^{-it\lambda_j},\ te^{-it\lambda_j}, \ldots,\ t^{N_j-1}e^{-it\lambda_j}. \tag{4}$$

Therefore, even if every eigenvalue λ_j is real, $e^{-it\mathscr{H}}$ can describe 'instabilities' (growth of oscillations). The algebraic growth of amplitudes (the factors t^p) is called 'secularity', which represents 'resonant' interactions of oscillators with a common frequency (degenerate eigenvalue). This 'resonance' must be distinguished from the so-called 'wave–particle resonance' (Cherenkov resonance) which results in the Landau (phase mixing) damping. The latter is also related to continuous spectra, while it is different from the process discussed here – wave–wave resonance among overlapping continuous spectra.

The analysis is much more complicated when frequency overlapping occurs in continuous spectra. As mentioned above, phase mixing due to continuous spectra brings about complex transient phenomena that are strongly dependent upon initial conditions. The present study focuses on the degeneracy of spectra between point and continuum, or continuum and continuum which has never been treated so far. Our analysis will show an interesting relation between the order of secularity and the number of degenerate (frequency-overlapping) spectra.

In Sec. 2, we begin by reviewing the general mathematical structure of continuous spectra associated with an ambient shear flow in a system of various waves. The convective derivatives produce essential singularity in the resolvent operator. Inhomogeneity of the flow also enables energy exchanges between fluctuations and the flow. This interaction does not allow a Hamiltonian representation – the energy is not conserved in the fluctuation parts of the fields. In Sec. 3, we introduce a simple model of a shear-flow system. A single species (non-neutral) plasma produces a shear

flow to be confined in a magnetic field. The so-called diocotron instability is an electrostatic analogue of the Kelvin–Helmholtz instability. When this exponential instability is stable, the corresponding eigenvalue (point spectrum) occurs in the region of the continuous spectrum (representing the shear flow) on the real axis. This 'frequency overlapping' causes degenerate spectra, and secular behavior stems from there. However, this secular growth saturates because of the mixing effect. In Sec. 4, we introduce another continuous spectrum caused by parallel (with respect to the magnetic field) motion of the plasma. The amplitude of the resonant 'local' mode increases algebraically. We will solve the initial value problem and show that an appropriate renormalization technique can predict the secular behavior of the local mode. We will compare the analytical result with our previous numerical simulation [2]. In Appendix A, we will confirm the validity of the renormalization method by comparing it with the conventional Laplace transform approach.

2. Non-Hermitian property of shear flow

In this section, we review the effects of shear flow and their mathematical representations. The simplest model of shear flow is the vortex dynamics in inviscid incompressible fluids,

$$\partial_t \mathbf{w} - \nabla \times (\mathbf{v} \times \mathbf{w}) = 0, \tag{5}$$

where $\mathbf{v}$ is the velocity and $\mathbf{w} = \nabla \times \mathbf{v}$ is the vorticity. In a two-dimensional space, we may write $\mathbf{v} = \nabla\psi(x, y) \times \nabla z$, and rewrite (5) in the form of a Liouville equation,

$$\partial_t w + \{\psi, w\} = 0, \tag{6}$$

where $w = -\Delta\psi$ is the z-component of $\mathbf{w}$, and $\{\psi, w\} = (\partial_y\psi)(\partial_x w) - (\partial_x\psi)(\partial_y w)$. By decomposing the equilibrium (capital letters) and fluctuation (tildes) parts, the linearized equation becomes

$$\partial_t \tilde{w} + \{\Psi, \tilde{w}\} + \{\tilde{\psi}, W\} = 0. \tag{7}$$

In a stratified shear flow $\mathbf{V} = (0, V_y(x), 0)$, we assume $\tilde{w}(x, y, t) = \tilde{w}(x, t)e^{-ik_y y}$ (k_y is a good quantum number). Then, (7) reduces into the Rayleigh equation [8]

$$-i\partial_t \tilde{w} - k_y V_y(x)\tilde{w} - k_y V_y''(x)\mathcal{G}_x\tilde{w} = 0, \tag{8}$$

where, considering the whole space (without boundary),

$$\mathcal{G}_x\tilde{w} := -\Delta^{-1}\tilde{w} = \frac{1}{2k_y}\int_{-\infty}^{\infty} e^{-k_y|x-\xi|}\tilde{w}(\xi)\,d\xi. \tag{9}$$

The third term on the left-hand side of (8) is the origin of the non-Hermitian property of the problem. If $V_y''(x)$ changes the sign (i.e. the flow $V_y(x)$ has inflection points), the generator of (8) cannot be a Hermitian operator in any definition of Hilbert space. Complex eigenvalues may occur, representing the Kelvin–Helmholtz (KH) instabilities. The second term on the left-hand side of (8), the convective derivative, produces a continuous spectrum [1] (replacing ∂_t by $i\omega$, the term $\omega - kV_y(x)$ yields an essential singularity in the formal dispersion relation). The phase-mixing effect due to the continuous spectrum, in addition to the non-Hermitian property, causes a rather complex evolution of the fluctuations. Possible instabilities associated with the continuous spectrum (Sec. 1) are in marked contrast with the KH instabilities – they are spatially localized, continuously changing the shape, and temporally algebraic.

A close cousin of the two-dimensional incompressible flow are the electrostatic perturbations in single-species plasma confined by a homogeneous magnetic field $\mathbf{B}$. The $\mathbf{E}\times\mathbf{B}$ drift velocity in the plane perpendicular to $\mathbf{B}$ can be written in the form $-\nabla\phi\times\mathbf{B}/B^2$. The Poisson equation implies that the vorticity $-\Delta\phi$ parallels the density of the non-neutral plasma.

In a more general system, other physical variables may couple with the vorticity. Let $\boldsymbol{\xi}$ be a state vector that is, in a plasma, a combination of the vorticity w, pressure p, density ρ, magnetic field $\mathbf{B}$ and so on. We decompose $\boldsymbol{\xi}$ into the equilibrium $\boldsymbol{\Xi}$ and fluctuation $\tilde{\boldsymbol{\xi}}$ parts. The transport equations (conservation laws) contain convective derivatives $[(\mathbf{v}\cdot\nabla)\boldsymbol{\xi}]$. The linearized evolution equations, in two-dimensional spaces, can be cast in the form of

$$\partial_t\tilde{\boldsymbol{\xi}}+\{\Psi,\tilde{\boldsymbol{\xi}}\}+\{\tilde{\psi},\boldsymbol{\Xi}\}=\mathscr{A}\,\tilde{\boldsymbol{\xi}}, \tag{10}$$

where $\mathscr{A}$ is a linear operator (including $\boldsymbol{\Xi}$). The non-diagonal components of $\mathscr{A}$ describe the couplings among different variables. If y is an ignorable coordinate of $\boldsymbol{\Xi}$, (10) translates (using a good quantum number k_y) into

$$-i\partial_t\tilde{\boldsymbol{\xi}}-k_yV_y(x)\tilde{\boldsymbol{\xi}}-k_y\boldsymbol{\Xi}'(x)\mathscr{G}_x\tilde{w}=-i\,\mathscr{A}\,\tilde{\boldsymbol{\xi}}. \tag{11}$$

The operator $[-i\partial_t-k_yV_y(x)]$ acting on all variables yields multiple (overlapped) continuous spectra. The aim of this paper is to analyze the secular behavior of perturbations stemming from this overlapped continuous spectra.

3. Rayleigh equation and phase-mixing effect

As the simplest example of the two-dimensional, shear-flow problem, we consider the Rayleigh equation (8) describing electrostatic fluctuations in a non-neutral (single species) plasma. In this model, we can observe the resonance between the point spectrum and the continuous spectrum.

Let $\mathbf{B}=(0,0,B_z)$ be a homogeneous magnetic field, which confines an electron plasma within slab geometry. We normalize the variables by choosing the representative density, magnetic field and length. We consider a simple flat top density

$$N(x)=\begin{cases}1 & |x|\leqslant 1\\ 0 & |x|>1,\end{cases} \tag{12}$$

which produces ambient shear flow

$$V_y(x)=\begin{cases}-1 & x<-1\\ x & -1<x<1\\ 1 & 1<x.\end{cases} \tag{13}$$

Let us Fourier-transform fluctuations with respect to y and z. If $k_z\neq 0$, the parallel (with respect to $\mathbf{B}$) plasma oscillation couples with the perpendicular vortex dynamics [2]. The determining equations are

$$i\partial_t\tilde{n}+k_yV_y\tilde{n}-k_yV_y''\tilde{\phi}+Nk_z\tilde{v}_z=0, \tag{14}$$

$$i\partial_t\tilde{v}_z+k_yV_y\tilde{v}_z=\frac{k_z}{s^2}\tilde{\phi}, \tag{15}$$

$$\tilde{\phi}=-\mathscr{G}_x\tilde{n}:=-\frac{1}{2k}\int_{-\infty}^{\infty}e^{-k|x-\xi|}\tilde{n}(\xi)\,d\xi, \tag{16}$$

where $k := \sqrt{k_y^2 + k_z^2}$ and $s := \omega_{\rm p}/\omega_{\rm c}$ (with $\omega_{\rm p}$ = plasma frequency and $\omega_{\rm c}$ = cyclotron frequency). We assume $s \ll 1$ (implying low density).

If $k_z = 0$, (14) and (15) are decoupled. The KH instability predicted by the standard Rayleigh equation (14) is the so-called diocotron instability [9, 10]. In this section, we revisit the Rayleigh equation (assuming $k_z = 0$) to highlight the non-Hermitian property. Oblique modes ($k_z \neq 0$) will be discussed in Sec. 4.

By (13), we observe that

$$V_y''(x) = \delta(x+1) - \delta(x-1). \tag{17}$$

Therefore, the perturbed density (vorticity) must include delta functions,

$$\tilde{n}(x,t) = a(t)\delta(x+1) + b(t)\delta(x-1) + f(x,t), \tag{18}$$

where $f(x,t)$ is the smooth part of the fluctuation, while the delta functions represent the 'surface waves'. Substituting (18) into the Rayleigh equation (14) (with $k_z = 0$), we obtain

$$-i\partial_t \begin{pmatrix} f(x) \\ a \\ b \end{pmatrix} = \begin{pmatrix} k_y x & 0 & 0 \\ k_y \mathscr{G}_{-1} & -\frac{1}{2}(2k_y - 1) & \frac{1}{2}e^{-2k_y} \\ -k_y \mathscr{G}_1 & -\frac{1}{2}e^{-2k_y} & \frac{1}{2}(2k_y - 1) \end{pmatrix} \begin{pmatrix} f(x) \\ a \\ b \end{pmatrix}. \tag{19}$$

The coupling of a and b determines the two-point spectrum [8–11],

$$\omega_\pm = \pm\tfrac{1}{2}\sqrt{(2k_y - 1)^2 - e^{-4k_y}}\,. \tag{20}$$

By equating the right-hand side of (20) to zero, we obtain a critical wave number $k_{\rm c} \simeq 0.639$. For $k_y < k_{\rm c}$, the frequencies $\omega_\pm$ assume pure imaginary numbers, representing the KH instability. The corresponding eigenfunctions are

$$\begin{pmatrix} f_{\omega_\pm}(x) \\ a_{\omega_\pm} \\ b_{\omega_\pm} \end{pmatrix} = \begin{pmatrix} 0 \\ e^{-2k_y} \\ (2k_y - 1) + 2\omega_\pm \end{pmatrix}. \tag{21}$$

On the other hand, the continuous part $f(x,t)$ receives phase mixing that is represented by the continuous spectrum $\sigma_{\rm c} = \{\omega \in \mathbb{R}; -k_y < \omega < k_y\}$. The corresponding singular eigenfunction is formally written as

$$\begin{aligned} &f_\omega(x) = \delta(\omega - k_y x), \\ &\begin{pmatrix} a_\omega \\ b_\omega \end{pmatrix} = \frac{1}{(\omega - \omega_+)(\omega - \omega_-)} \begin{pmatrix} \omega - \frac{1}{2}(2k_y - 1) & \frac{1}{2}e^{-2k_y} \\ -\frac{1}{2}e^{-2k_y} & \omega + \frac{1}{2}(2k_y - 1) \end{pmatrix} \\ &\qquad \times \begin{pmatrix} \dfrac{1}{2k_y} e^{-(k_y + \omega)} \\ -\dfrac{1}{2k_y} e^{-(k_y - \omega)} \end{pmatrix}. \end{aligned} \tag{22}$$

A flat top density $\partial N/\partial x = 0$, as assumed in this paper, yields the real point spectra (20) for $k_y \geqslant k_{\rm c}$. Then, we fail to derive the singular eigenfunction with the frequency $\omega = \omega_+$ or $\omega = \omega_-$ in the expression of (22), and have to find a generalized singular eigenfunction (nilpotent), which constructs a Jordan block. This Jordan block represents the 'resonance' in the overlapping spectra. Using (21),

the generalized eigenfunctions are calculated as

$$\hat{f}_{\omega_\pm} = \hat{c}_{\omega_\pm}\delta(\omega_\pm - k_y x),$$

$$\begin{pmatrix}\hat{c}_{\omega_\pm}\\ \hat{a}_{\omega_\pm}\end{pmatrix} = \begin{pmatrix} -\dfrac{1}{2k_y}e^{-(k_y+\omega_\pm)} & \omega_\pm + \frac{1}{2}(2k_y-1)\\ \dfrac{1}{2k_y}e^{-(k_y-\omega_\pm)} & \frac{1}{2}e^{-2k_y}\end{pmatrix}^{-1}\begin{pmatrix}a_{\omega_\pm}\\ b_{\omega_\pm}\end{pmatrix}, \tag{23}$$

$$\hat{b}_{\omega_\pm} = 0,$$

where we have chosen $\hat{b}_{\omega_\pm} = 0$ for simplicity. Note that one may add (21) with the multiplication of an arbitrary constant to the expression (23).

In the analogy of linear algebra, one may expect a secular behavior of the KH mode (21), such as $te^{i\omega_\pm t}$ (see (4)). However, we do not observe secular behavior – an essential difference of infinite dimensional Hilbert space from linear algebra. This is due to the phase mixing in the continuous spectrum. Let us demonstrate this fact by solving the initial value problem.

Since the evolution of f is independent of a and b, we readily obtain the general solution of f,

$$f(x,t) = f(x,0)e^{ik_y xt}. \tag{24}$$

The general solutions of a and b are given by the Duhamel formula,

$$\begin{aligned}\begin{pmatrix}a(t)\\ b(t)\end{pmatrix} &= \mathbf{T}\begin{pmatrix}e^{i\omega_+ t} & 0\\ 0 & e^{i\omega_- t}\end{pmatrix}\mathbf{T}^{-1}\begin{pmatrix}a(0)\\ b(0)\end{pmatrix}\\ &\quad + \mathbf{T}\begin{pmatrix}e^{i\omega_+ t} & 0\\ 0 & e^{i\omega_- t}\end{pmatrix}\\ &\quad \times \int_0^t \begin{pmatrix}e^{-i\omega_+ t'} & 0\\ 0 & e^{-i\omega_- t'}\end{pmatrix}\mathbf{T}^{-1}\begin{pmatrix}ik_y(\mathscr{G}_{-1}f)(t')\\ -ik_y(\mathscr{G}_1 f)(t')\end{pmatrix}dt',\end{aligned} \tag{25}$$

where

$$\mathbf{T} = \begin{pmatrix}a_{\omega_+} & a_{\omega_-}\\ b_{\omega_+} & b_{\omega_-}\end{pmatrix}. \tag{26}$$

If $\omega_\pm \in \mathbb{R}$ (stable KH modes), the first term of the right-hand side of (25) describes harmonic oscillation. The second term needs careful treatment.

We observe that

$$(\mathscr{G}_x f)(t) = \frac{1}{2k_y}\int_{-\infty}^{\infty} e^{-k_y|x-\xi|}f(\xi,0)e^{ik_y\xi t}\,d\xi, \tag{27}$$

$$= \int_{-\infty}^{\infty} g(x,\check{\xi})e^{i\check{\xi}t}\,d\check{\xi}, \tag{28}$$

where $\check{\xi} := k_y\xi$ and

$$g(x,\check{\xi}) := \frac{1}{2k_y^2}e^{-|k_y x-\check{\xi}|}f(\check{\xi}/k_y,0). \tag{29}$$

Equation (28) is the Fourier transform ($\check{\xi}\to t$) of $g(x,\check{\xi})$. If $|g(x,\check{\xi})|$ is integrable with respect to $\check{\xi}$, the Riemann–Lebesgue theorem shows that $\lim_{t\to\pm\infty}\mathscr{G}_x f = 0$, implying the phase mixing damping.

Because the integrants $\mathscr{G}_{\pm 1} f(t')$ are decreasing functions of t', they do not include stationary oscillations $e^{i\omega_\pm t'}$. Therefore, the second term of (25) does not diverge at the limit of $t \to \infty$. We, thus, find that the resonance between the continuous spectrum and the point spectrum does not result in an algebraic instability – the phase mixing overcomes the resonant amplification.

In the present work, we assume a flat top density. If the equilibrium density has a gradient, the real point spectra convert either to real continuous spectra or to unstable ($\mathrm{Im}(\omega) > 0$) complex point spectra, depending on the sign of the density gradient [9, 12]. Briggs et al. [12] have pointed out that a positive density gradient gives rise to the exponential growth of the diocotron wave, i.e. a complex point spectrum is created. This exponential instability is distinguished from the present secular behavior caused by frequency overlapping among the real point spectrum and continuous spectrum. On the other hand, the point spectrum disappears in the presence of a negative density gradient. Potential fluctuations undergo phase mixing and damping.

4. Coupled continuous spectra and algebraic instabilities

In Sec. 3, we have considered the Rayleigh equation (14) governing the perturbations in the plane perpendicular to the ambient magnetic field. In this section, we consider the parallel motion (15) and the coupling between the parallel and perpendicular modes. If $k_z = 0$ (decoupled), (15) becomes

$$i\partial_t \tilde{v}_z + k_y V_y \tilde{v}_z = 0, \tag{30}$$

which has a continuous spectrum $\sigma_c = \{\omega \in \mathbb{R}; -k_y < \omega < k_y\}$ due to the shear flow $V_y(x) = x$ $(-1 < x < 1)$. The corresponding singular eigenfunction is

$$\tilde{v}_{z\omega}(x) = \delta(\omega - k_y x). \tag{31}$$

This continuous spectrum overlaps with that of perpendicular motion.

Since a finite k_z yields a coupling of (14) and (15), the resonance of two continuous spectra occurs. We rewrite (14)–(16) in matrix form,

$$-i\frac{\partial}{\partial t}\begin{pmatrix} f(x) \\ \tilde{v}_z(x) \\ a \\ b \end{pmatrix} = \mathscr{A}\begin{pmatrix} f(x) \\ \tilde{v}_z(x) \\ a \\ b \end{pmatrix}, \tag{32}$$

where the generator is

$$\mathscr{A} := \begin{pmatrix} k_y x & k_z & 0 & 0 \\ \dfrac{k_z}{s^2}\mathscr{G}_x & k_y x & \dfrac{k_z}{2ks^2}e^{-k|x+1|} & \dfrac{k_z}{2ks^2}e^{-k|x-1|} \\ k_y \mathscr{G}_{-1} & 0 & -\dfrac{k_y}{2k}(2k-1) & \dfrac{k_y}{2k}e^{-2k} \\ -k_y \mathscr{G}_1 & 0 & -\dfrac{k_y}{2k}e^{-2k} & \dfrac{k_y}{2k}(2k-1) \end{pmatrix}. \tag{33}$$

Spectral analysis [13] shows that exponential instabilities (ω with an imaginary part) are removed if $k_z \neq 0$ and s^2 is sufficiently small. However, numerical solutions of the initial value problem show that oscillations grow in proportion to t near the 'resonant surfaces' ($x = \mu_\pm := \omega_\pm / k_y$) when $k_y \gg k_z \sim O(s)$ [2] (see Sec. 4.3).

Since the phase mixing diminishes the magnitude of the convolution integral $\mathscr{G}_x f$, the first approximation one may consider is to neglect the $\mathscr{G}_x f$ terms in the generator $\mathscr{A}$ [2]. Then, (32) gives a (3×3) Jordan block. This approximation yields parabolical growth ($\propto t^2$) in the amplitude of $f(\mu_+)$, which does not agree with the numerical result ($\propto t$).

This discrepancy is due to the neglect of $\mathscr{G}_x f$. Because $\lim_{t\to\infty} f(x,t)$ is singular, we need a careful treatment of the integral terms $\mathscr{G}_x f$. In the following subsections, we shall solve the initial value problem and study the asymptotic behavior invoking a renormalization method.

4.1. Renormalized perturbation theory (multiple-scale analysis)

We assume $\epsilon = k_z = O(s^2)$ is a small parameter, and consider two time scales,

$$\tau = t, \quad T = \epsilon t. \tag{34}$$

The independent variables are expanded as

$$f(x,t) = \sum_{n=0}^{\infty} \epsilon^n f_n(x,\tau,T), \tag{35}$$

$$\tilde{v}_z(x,t) = \sum_{n=0}^{\infty} \epsilon^n \tilde{v}_{zn}(x,\tau,T), \tag{36}$$

$$a(t) = \sum_{n=0}^{\infty} \epsilon^n a_n(\tau,T), \tag{37}$$

$$b(t) = \sum_{n=0}^{\infty} \epsilon^n b_n(\tau,T). \tag{38}$$

Using the relation

$$\frac{\partial}{\partial t} = \frac{\partial}{\partial \tau} + \epsilon \frac{\partial}{\partial T}, \tag{39}$$

(32) reads

$$-i\frac{\partial}{\partial \tau}\begin{pmatrix} f(x) \\ \tilde{v}_z(x) \\ a \\ b \end{pmatrix} = \mathscr{A}\begin{pmatrix} f(x) \\ \tilde{v}_z(x) \\ a \\ b \end{pmatrix} + i\epsilon\frac{\partial}{\partial T}\begin{pmatrix} f(x) \\ \tilde{v}_z(x) \\ a \\ b \end{pmatrix}. \tag{40}$$

Substituting (35)–(38) into (40), we can solve these equations successively in the order of ϵ^0, ϵ^1, $\epsilon^2, \ldots$.

To simplify the analysis, we consider a specific initial condition

$$f(x,0) = 0, \quad \tilde{v}_z(x,0) = 0, \quad a(0) = e^{-2k}, \quad b(0) = \kappa_+, \tag{41}$$

where κ_+ is a constant to be determined later in (46).

f_0 obeys

$$-i\frac{\partial f_0}{\partial \tau} = k_y x f_0, \tag{42}$$

which yields $f_0(x,\tau,T) \equiv 0$. Then, a_0 and b_0 satisfy

$$-i\frac{\partial}{\partial \tau}\begin{pmatrix} a_0 \\ b_0 \end{pmatrix} = \frac{k_y}{2k}\begin{pmatrix} -2k+1 & e^{-2k} \\ -e^{-2k} & 2k-1 \end{pmatrix}\begin{pmatrix} a_0 \\ b_0 \end{pmatrix}. \tag{43}$$

The solution is

$$a_0(\tau,T)=A(T)e^{-2k}e^{i\omega_+\tau},\quad b_0(\tau,T)=A(T)\kappa_+e^{i\omega_+\tau}, \tag{44}$$

where

$$\omega_\pm:=\pm\frac{k_y}{2k}\sqrt{(2k-1)^2-e^{-4k}}, \tag{45}$$

$$\kappa_\pm:=(2k-1)\pm\sqrt{(2k-1)^2-e^{-4k}}. \tag{46}$$

The amplitude $A(T)$ is a certain function satisfying $A(0)=1$. The slow evolution of $A(T)$ will be determined later.

The short-term equation of $\tilde{v}_{z0}$ is

$$-i\frac{\partial\tilde{v}_{z0}}{\partial\tau}=k_yx\tilde{v}_{z0}+A(T)q(x)e^{i\omega_+\tau}, \tag{47}$$

which gives

$$\tilde{v}_{z0}(x,\tau,T)=A(T)q(x)e^{i\omega_+\tau}\frac{1-e^{-iU(x)\tau}}{U(x)}, \tag{48}$$

where

$$q(x):=\frac{k_z}{2ks^2}\big(e^{-k(x+1)}e^{-2k}+e^{-k(1-x)}\kappa_+\big), \tag{49}$$

$$U(x):=\omega_+-k_yx. \tag{50}$$

At the resonant surface ($x=\mu_+:=\omega_+/k_y$), $\tilde{v}_{z0}$ is secular ($\propto\tau$). Using $\tilde{v}_{z0}$, we may determine the short-term behavior of f_1 by

$$-i\frac{\partial f_1}{\partial\tau}=k_yxf_1+\tilde{v}_{z0}, \tag{51}$$

which yields

$$f_1(x,\tau,T)=A(T)q(x)e^{i\omega_+\tau}\frac{\big[\big(1-e^{-iU(x)\tau}\big)/U(x)\big]-i\tau e^{-iU(x)\tau}}{U(x)}. \tag{52}$$

This f_1 is also secular ($\propto\tau^2$) at the resonant surface ($x=\mu_+$). As mentioned above, the estimate of the power of the secularity disagrees with the numerical observation. The slow variable $A(T)$ will amend the long-term behavior.

We proceed to the equations of a_1 and b_1:

$$\begin{aligned}-i\frac{\partial}{\partial\tau}\begin{pmatrix}a_1\\b_1\end{pmatrix}&=\frac{k_y}{2k}\begin{pmatrix}-2k+1 & e^{-2k}\\ -e^{-2k} & 2k-1\end{pmatrix}\begin{pmatrix}a_1\\b_1\end{pmatrix}\\&\quad+k_y\begin{pmatrix}\mathscr{G}_{-1}f_1\\-\mathscr{G}_1f_1\end{pmatrix}+i\frac{\partial}{\partial T}\begin{pmatrix}a_0\\b_0\end{pmatrix}.\end{aligned} \tag{53}$$

By the transformation,

$$\begin{pmatrix}\hat{a}_1\\\hat{b}_1\end{pmatrix}:=\begin{pmatrix}e^{-2k} & e^{-2k}\\ \kappa_+ & \kappa_-\end{pmatrix}^{-1}\begin{pmatrix}a_1\\b_1\end{pmatrix}. \tag{54}$$

Equation (53) is diagonalized as

$$\frac{\partial}{\partial\tau}\begin{pmatrix}\hat{a}_1\\\hat{b}_1\end{pmatrix}=\begin{pmatrix}i\omega_+ & 0\\0 & i\omega_-\end{pmatrix}\begin{pmatrix}\hat{a}_1\\\hat{b}_1\end{pmatrix}+A(T)\begin{pmatrix}h_a(\tau)\\h_b(\tau)\end{pmatrix}-\frac{\partial}{\partial T}\begin{pmatrix}A(T)e^{i\omega_+\tau}\\0\end{pmatrix}, \tag{55}$$

where

$$\begin{pmatrix} h_a(\tau) \\ h_b(\tau) \end{pmatrix} := \frac{ik_y}{A(T)} \begin{pmatrix} e^{-2k} & e^{-2k} \\ \kappa_+ & \kappa_- \end{pmatrix}^{-1} \begin{pmatrix} \mathscr{G}_{-1} f_1 \\ -\mathscr{G}_1 f_1 \end{pmatrix}. \tag{56}$$

Since $f_1 \propto A(T)$, h_a and h_b are independent of T. The equation of $\hat{a}_1$ reads

$$\frac{\partial \hat{a}_1}{\partial \tau} = i\omega_+ \hat{a}_1 + A(T) h_a(\tau) - \frac{dA}{dT} e^{i\omega_+ \tau}. \tag{57}$$

If $h_a(\tau)$ includes an oscillation with frequency ω_+, i.e.

$$h_a(\tau) = \sigma e^{i\omega_+ \tau} + \cdots \quad (\sigma = \text{const}), \tag{58}$$

$\hat{a}_1$ becomes a secular solution. We may remove this divergence by imposing a renormalization group equation

$$\sigma A(T) - \frac{dA}{dT} = 0, \tag{59}$$

which gives

$$A(T) = e^{\sigma T}. \tag{60}$$

We have derived the renormalized solution

$$\hat{a}_0 = e^{\sigma T} e^{i\omega_+ \tau}, \tag{61}$$

$$= e^{\sigma \epsilon t} e^{i\omega_+ t}, \tag{62}$$

$$= e^{\sigma k_z t} e^{i\omega_+ t}. \tag{63}$$

If the real part of σk_z is negative, this solution represents the damping of $\hat{a}$.

4.2. Fourier expansion

Let us proceed to estimate the 'Fourier coefficient' σ defined by

$$\sigma := \lim_{t' \to \infty} \frac{1}{t'} \int_0^{t'} h_a(t) e^{-i\omega_+ t}\, dt. \tag{64}$$

By (52) and (56), we obtain

$$h_a(t) = -iCe^{i\omega_+ t} \int_{-1}^{1} (2e^{-2k} + \kappa_- e^{-2k\xi} + \kappa_+ e^{2k\xi}) \times \frac{\left[\left(1 - e^{-iU(\xi)t}\right)/U(\xi)\right] - ite^{-iU(\xi)t}}{U(\xi)}\, d\xi, \tag{65}$$

$$C := \frac{k_z k_y e^{-2k}}{4k^2 s^2 (\kappa_+ - \kappa_-)}. \tag{66}$$

We may write

$$\begin{aligned} h_a(t) e^{-i\omega_+ t} &= iC \int_{-1}^{1} (2e^{-2k} + \kappa_- e^{-2k\xi} + \kappa_+ e^{2k\xi}) \int_0^t \zeta e^{-iU(\xi)\zeta}\, d\zeta\, d\xi, \\ &= C \frac{2e^{-2k}}{k_y} \int_0^t \left[e^{i(-\omega_+ + k_y)\zeta} - e^{i(-\omega_+ - k_y)\zeta} \right] d\zeta \\ &\quad + iC\kappa_- \int_0^t \zeta \frac{e^{-2k + i(-\omega_+ + k_y)\zeta} - e^{2k + i(-\omega_+ - k_y)\zeta}}{-2k + ik_y\zeta}\, d\zeta \\ &\quad + iC\kappa_+ \int_0^t \zeta \frac{e^{2k + i(-\omega_+ + k_y)\zeta} - e^{-2k + i(-\omega_+ - k_y)\zeta}}{2k + ik_y\zeta}\, d\zeta. \end{aligned} \tag{67}$$

Using the relations

$$\int_0^\infty \frac{\cos(\beta x)}{\alpha^2+x^2}\,dx = \frac{\pi}{2|\alpha|}e^{-|\alpha||\beta|}, \quad \int_0^\infty \frac{x\sin(\beta x)}{\alpha^2+x^2}\,dx = \frac{\pi\beta}{2|\beta|}e^{-|\alpha||\beta|} \quad (\forall\alpha,\beta\in\mathbb{R}) \tag{68}$$

we observe, for large t,

$$\mathrm{Im}\left(\int_0^t x\frac{e^{i\beta x}}{\alpha+ix}\,dx\right) \simeq -\frac{\sin(\beta t)}{\beta} + \alpha\left(\frac{\alpha}{|\alpha|}+\frac{\beta}{|\beta|}\right)\frac{\pi}{2}e^{-|\alpha||\beta|}. \tag{69}$$

Using (69) in (67) yields, for large t,

$$\begin{aligned}\mathrm{Re}(h_a(t)e^{-i\omega_+ t}) \simeq\ & C\frac{1}{k_y}(2e^{-2k}+\kappa_- e^{-2k}+\kappa_+ e^{2k})\frac{\sin(-\omega_+ + k_y)t}{(-\omega_+ + k_y)} \\ & - C\frac{1}{k_y}(2e^{-2k}+\kappa_- e^{2k}+\kappa_+ e^{-2k})\frac{\sin(-\omega_+ - k_y)t}{(-\omega_+ - k_y)} \\ & + C\frac{2k\pi}{k_y|k_y|}\left(\kappa_- e^{-(2k/k_y)\omega_+} - \kappa_+ e^{(2k/k_y)\omega_+}\right).\end{aligned} \tag{70}$$

Substituting (70) into (64), we find that the third term on the right-hand side of (70) yields the real part of σ:

$$\mathrm{Re}(\sigma) = \frac{k_z\pi e^{-2k}}{2ks^2|k_y|(\kappa_+-\kappa_-)}\left(\kappa_- e^{-(2k/k_y)\omega_+} - \kappa_+ e^{(2k/k_y)\omega_+}\right). \tag{71}$$

In the stable regime of the KH modes ($k_y > k_c$), (71) is simplified as

$$\mathrm{Re}(\sigma) \simeq -\frac{k_z\pi}{2k_y^2 s^2 e} \quad (<0). \tag{72}$$

We have derived the damping rate of $\hat{a}$ (see (63)):

$$\nu = -\mathrm{Re}(\sigma)k_z, \tag{73}$$

$$\simeq \frac{k_z^2\pi}{2k_y^2 s^2 e}. \tag{74}$$

The asymptotic form of $\hat{a}$ is

$$\hat{a}(t) = e^{(i\omega_+ - \nu)t}. \tag{75}$$

4.3. Comparison with numerical solution

In this subsection, we compare the analytical result with numerical simulation. We use the trapezoidal rule for spatial integration. Because of the continuous spectrum, a solution receives the mixing effect (see (24)). $f(x,t)$ becomes strongly oscillatory as t increases. The wave number with respect to x is of order $k_y t$. For the range of $t<T$, we choose the mesh number per unit length (N_{mesh}) to satisfy $N_{\mathrm{mesh}} \gg k_y T$.

For numerical example, let us take $k_y = 1, k_z = 10^{-3}$ and $s = 10^{-2}$. Then, (74) yields $\nu \simeq 0.005\,78$. This analytical estimate is compared with numerical simulation. By substituting the initial condition (41), we observe the secularity at $x=\mu_+$ (see Fig. 1). The time evolution of $a(t)$ shows damping which seems to be exponential (Fig. 2(a)). In Fig. 3, we compare the analytical ν (given by (74)) and the numerically estimated damping rate (k_y is the parameter).

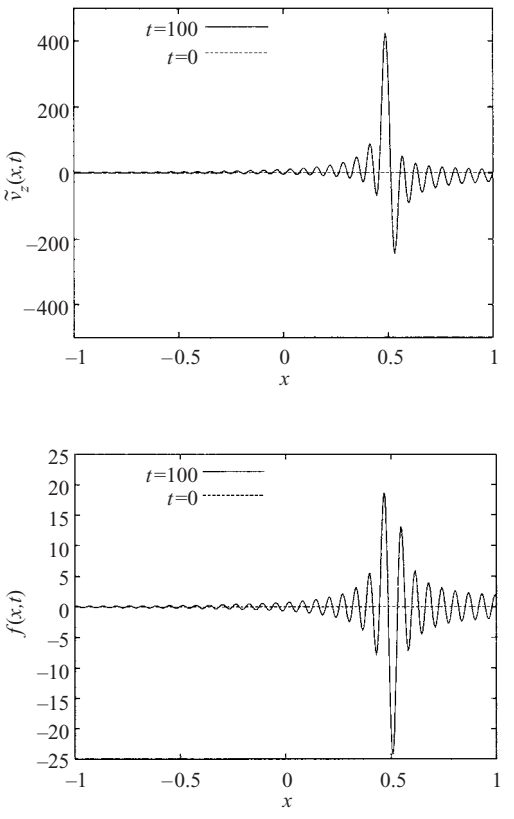

Figure 1. Profiles of $\tilde{v}_z(x,t)$ and $f(x,t)$ at $t=100$. The parameters are $k_y=1$, $k_z=10^{-3}$, $s=10^{-2}$, and the initial condition is given by (41). Near the resonant surface ($x=\mu_+=0.495$), large oscillations appear.

By substituting $A(T)=e^{-\nu t}$ into (47) and (51), we obtain

$$\tilde{v}_z(x,t) \simeq \tilde{v}_{z0} = iq(x)e^{ik_y xt}\frac{e^{(iU(x)-\nu)t}-1}{iU(x)-\nu}, \tag{76}$$

$$f(x,t) \simeq \epsilon f_1 = k_z q(x)e^{ik_y xt}\frac{\left[\left(1-e^{(iU(x)-\nu)t}\right)/(iU(x)-\nu)\right]+t}{iU(x)-\nu}. \tag{77}$$

We thus predict the saturation of $\tilde{v}_z(\mu_+,t)$ and the growth of $f(\mu_+,t)$ in proportion to t (see the dashed lines in Figs 2(b) and 2(c)). The remaining small error may be eliminated if we analyze the slow variations of $\tilde{v}_{z0}$ and f_1.

5. Summary

In a non-Hermitian system, degenerate spectra (frequency overlapping) may cause nilpotent, resulting in secular amplification of even real frequency waves. If ω is a degenerate point spectrum (eigenvalue) of nullity n, the corresponding Jordan block of dimension $(n+1)$ produces oscillations in the form of $e^{i\omega t}, te^{i\omega t}, \ldots, t^n e^{i\omega t}$. This elementary result does not apply when we consider degenerate 'continuous' spectra. We chose a single-species (non-neutral) plasma as a physical model for investigation.

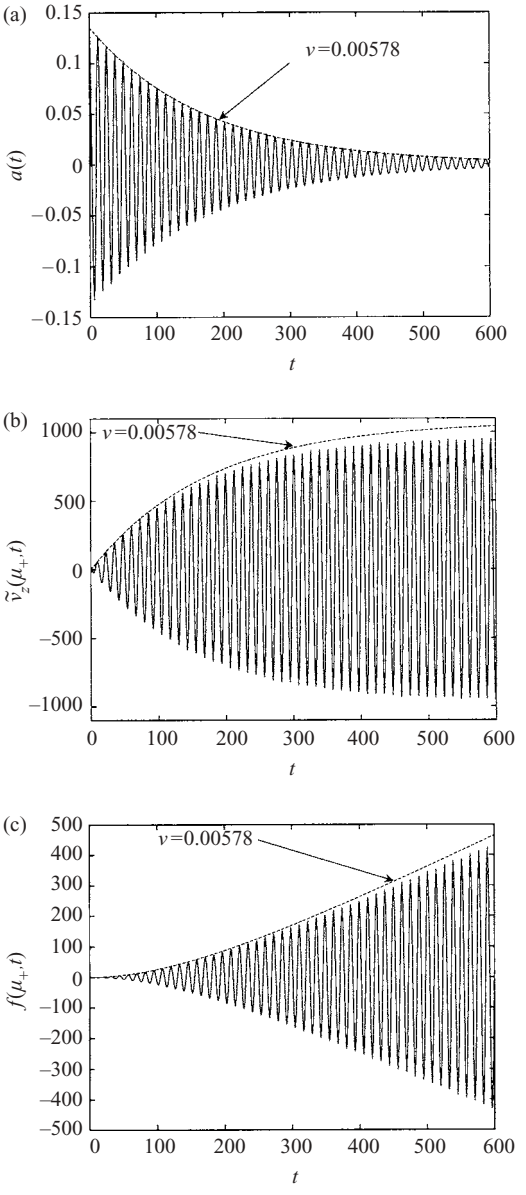

Figure 2. Time evolution of (a) the surface density fluctuation $a(t)$, (b) the parallel electron velocity $\tilde{v}_z(x,t)$ at $x = \mu_+$ (resonant surface) and (c) the inner density fluctuation $f(x,t)$ at $x = \mu_+$. The parameters are $k_y = 1$, $k_z = 10^{-3}$, $s = 10^{-2}$, and the initial condition is given by (41). Dashed lines denote the amplitudes of the analytical solutions (75)–(77), respectively.

The self-electric field yields an ambient shear flow that brings about continuous spectra (representing the convection of fluctuations) as well as non-Hermitian properties (interaction of fluctuations and the ambient flow). If a point spectrum ω overlaps with other m continuous spectra (i.e. formal nullity is $n = m + 1$), we obtain secularity of the form of $e^{i\omega t}, te^{i\omega t}, \ldots, t^m e^{i\omega t}$. The diminution of the power

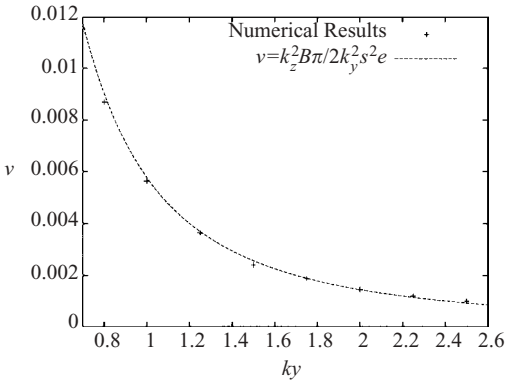

Figure 3. Damping rate of the surface wave for $k_z = 0.001, s = 0.01$. The dotted line denotes the plot of (74), and points are estimated by the fitting of numerical results (Fig. 2(a)).

of t is due to the phase mixing in the continuous spectra. The resonance (frequency overlapping) of a point spectrum and multiple continuous spectra is the cause of secular behavior. This process may occur in many other shear-flow systems.

The present analysis predicts an algebraic instability in a KH (diocotron) stable non-neutral plasma. The instability stems from the coupling of perpendicular (with respect to the magnetic field) vortical motion and parallel plasma oscillation. The fluctuation is localized at the surface where the frequency (real) of the stable diocotron waves resonates with the flow continuum.

Acknowledgements

This work is partially supported by a Grant-in-Aid from the Japanese Ministry of Education, Culture, Sports, Science and Technology, No. 14102033 and No. 12780353.

Appendix A. Comparison with the Laplace transform approach

An alternative method to analyze the initial value problem is the use of the Laplace transform. For the model of Sec. 4, we can construct a Green function to solve the transformed equation. Let us write

$$\tilde{\phi}_p(x) = \int_0^\infty \tilde{\phi}(x,t)e^{-pt}\,dt. \tag{A 1}$$

Equation (32) translates as

$$\tilde{\phi}_p'' - k^2\tilde{\phi}_p + \frac{k_z^2}{s^2(ip+k_yx)^2}\tilde{\phi}_p = -\frac{if(x,0)}{ip+k_yx} + \frac{ik_z\tilde{v}_z(x,0)}{(ip+k_yx)^2}. \tag{A 2}$$

The boundary conditions read

$$-(ip-k_y)\tilde{\phi}_p'(-1) + [k_y + k(ip-k_y)]\tilde{\phi}_p(-1) = ia(0), \tag{A 3}$$

$$-(ip+k_y)\tilde{\phi}_p'(1) + [k_y - k(ip+k_y)]\tilde{\phi}_p(1) = -ib(0), \tag{A 4}$$

where $f(x,0)$, $\tilde{v}_z(x,0)$, $a(0)$ and $b(0)$ denote the initial values of the corresponding variables. We assume the same initial values as (41). Then, the general solution of

(A 2) is

$$\tilde{\phi}_p(x) = C_1 \chi^{\frac{1}{2}} I_{-\eta}(\chi) + C_2 \chi^{\frac{1}{2}} I_{\eta}(\chi), \tag{A 5}$$

where $\chi := k(ip + k_y x)/k_y$, $\eta := \sqrt{1/4 - (k_z/sk_y)^2}$ and $I_{\pm\eta}(\chi)$ denotes the modified Bessel function. Substituting (A 5) into the boundary conditions (A 3) and (A 4), we can determine the coefficients C_1 and C_2:

$$\begin{pmatrix} C_1 \\ C_2 \end{pmatrix} = \frac{1}{k_y D(p,\eta)} \begin{pmatrix} \varphi_{11}(p,\eta) & \varphi_{12}(p,\eta) \\ \varphi_{21}(p,\eta) & \varphi_{22}(p,\eta) \end{pmatrix} \begin{pmatrix} ia(0) \\ -ib(0) \end{pmatrix}, \tag{A 6}$$

where

$$\varphi_{11}(p,\eta) = \left[-\chi \frac{\partial}{\partial \chi} \left(\chi^{\frac{1}{2}} I_{\eta}(\chi) \right) + (1-\chi) \chi^{\frac{1}{2}} I_{\eta}(\chi) \right]_{x=1}, \tag{A 7}$$

$$\varphi_{12}(p,\eta) = \left[\chi \frac{\partial}{\partial \chi} \left(\chi^{\frac{1}{2}} I_{\eta}(\chi) \right) - (1+\chi) \chi^{\frac{1}{2}} I_{\eta}(\chi) \right]_{x=-1}, \tag{A 8}$$

$$\varphi_{21}(p,\eta) = -\varphi_{11}(p,-\eta), \tag{A 9}$$

$$\varphi_{22}(p,\eta) = -\varphi_{12}(p,-\eta), \tag{A 10}$$

$$D(p,\eta) = \varphi_{11}(p,\eta)\varphi_{22}(p,\eta) - \varphi_{12}(p,\eta)\varphi_{21}(p,\eta). \tag{A 11}$$

If $k_z = 0$ (i.e. $\eta = 1/2$), we find $D(p_{\pm}, 1/2) = 0$, where $p = p_{\pm} (= i\omega_{\pm})$ are the poles of $\tilde{\phi}_p$ representing the KH modes. A small k_z (we write $\eta = 1/2 + \delta\eta$) moves the poles; $p = p_{\pm} + \delta p_{\pm}$. To calculate $\delta p_{\pm}$, we need the analytical continuation of $D(p,\eta)$ into the left-half plane of complex p, because $D(p,\eta)$ is a multivalued function when $\eta \neq 1/2$. We approximate $D(p,\eta)$ by

$$D(p,\eta) \simeq D(p_{\pm},1/2) + \delta p_{\pm} \frac{\partial D}{\partial p}(p_{\pm},1/2) + \delta\eta \frac{\partial D}{\partial \eta}(p_{\pm},1/2). \tag{A 12}$$

By setting $D(p,\eta) = 0$, we obtain

$$\delta p_{\pm} = -\delta\eta \frac{\frac{\partial D}{\partial \eta}(p_{\pm},1/2)}{\frac{\partial D}{\partial p}(p_{\pm},1/2)}. \tag{A 13}$$

After some manipulations, we find, for $k_y \gg k_z$,

$$\mathrm{Re}(\delta p_{\pm}) \simeq -\frac{k_z^2 \pi}{2k_y^2 s^2 e}. \tag{A 14}$$

Therefore, we find that both KH modes damp in the presence of a small k_z. The damping rate agrees with (74).

Since the modified Bessel function $I_{\pm\eta}(\chi)$ is described by $\chi^{\pm\eta}$ multiplied by an analytic function, the term with the strongest singularity in $\tilde{\phi}_p(x)$ is $\chi^{\frac{1}{2}-\eta} = (ip + k_y x)^{-\delta\eta}$. By operating the Laplacian ($\Delta = \partial^2/\partial x^2 - k^2$) on (A 5), the Laplace transform of the density perturbation ($\tilde{n}_p(x) = \Delta\tilde{\phi}_p(x)$ may include a singularity of the form of $(ip + k_y x)^{-2-\delta\eta}$, the x-dependence of which represents the continuous spectrum. The inverse Laplace transform, then, yields secular behavior [14]:

$$\tilde{n}(x,t) \sim t^{1+\delta\eta} e^{ik_y x t} \quad (t \to \infty). \tag{A 15}$$

All other contributions from lower-order singularities yield slower growth that can be neglected at large t. In (77), the small correction $\delta\eta$ for the power of t was also ignored.

References

[1] Case, K. M. 1960 Stability of inviscid plane Couette flow. *Phys. Fluids* **3**, 143.

[2] Hirota, M., Tatsuno, T., Kondoh, S. and Yoshida, Z. 2002 Secular behavior of electrostatic Kelvin–Helmholtz (diocotron) modes coupled with plasma oscillations. *Phys. Plasmas* **9**, 1177.

[3] Van Kampen, N. G. 1955 On the theory of stationary waves in plasmas. *Physica* **21**, 949.

[4] Case, K. M. 1959 Plasma Oscillations. *Ann. Phys.* **7**, 349.

[5] Smith, R. A. and Rosenbluth, M. N. 1990 Algebraic instability of hollow electron columns and cylindrical vortices. *Phys. Rev. Lett.* **64**, 649.

[6] Volponi, F., Yoshida, Z. and Tatsuno, T. 2000 Shear-flow induced stabilization of kinklike modes. *Phys. Plasmas* **7**, 2314.

[7] Tatsuno, T., Volponi, F. and Yoshida, Z. 2001 Transient phenomena and secularity of linear interchange instabilities with shear flows in homogeneous magnetic field plasmas. *Phys. Plasmas* **8**, 399.

[8] Rayleigh, J. W. S. 1880 On the stability, or instability, of certain fluid motions. *Proc. Lond. Math. Soc.* **9**, 57.

[9] Davidson, R. C. 1990 *Physics of Nonneutral Plasmas*. Redwood: Addison-Wesley, California.

[10] Hasegawa, A. 1975 *Plasma Instabilities and Nonlinear Effects*. Berlin: Springer-Verlag, p. 129.

[11] Chandrasekhar, S. 1961 *Hydrodynamic and Hydromagnetic Stability*. New York: Dover.

[12] Briggs, R. J., Daugherty, J. D. and Levy, R. H. 1970 Role of Landau damping in crossed-field electron beams and inviscid shear flow. *Phys. Fluids* **13**, 421.

[13] Kondoh, S., Tatsuno, T. and Yoshida, Z. 2001 Stabilization effect of magnetic shear on the diocotron instability. *Phys. Plasmas* **8**, 2635.

[14] Lighthill, M. J. 1958 *Introduction to Fourier Analysis and Generalized Functions*. Cambridge University Press, Cambridge, England.